



Cite this: *Chem. Commun.*, 2016, 52, 11096

Received 3rd June 2016,
Accepted 10th August 2016

DOI: 10.1039/c6cc04649e

www.rsc.org/chemcomm

Structural and mechanistic insights into a *Bacteroides vulgatus* retaining *N*-acetyl- β -galactosaminidase that uses neighbouring group participation†

C. Roth,^a M. Petricevic,^b A. John,^{cd} E. D. Goddard-Borger,^{*cd} G. J. Davies^{*a} and S. J. Williams^{*b}

***Bacteroides vulgatus* is a member of the human microbiota whose abundance is increased in patients with Crohn's disease. We show that a *B. vulgatus* glycoside hydrolase from the carbohydrate active enzyme family GH123, BvGH123, is an *N*-acetyl- β -galactosaminidase that acts with retention of stereochemistry, and, through a 3-D structure in complex with Gal-thiazoline, provide evidence in support of a neighbouring group participation mechanism.**

The human gastrointestinal tract undergoes a constant process of renewal, leading to production of 5×10^7 cells per minute and the discharge of 250 g of cells per day.¹ Colonocytes derived from the epithelia of the large intestine can be isolated at concentrations of up to 10^7 per gram of wet fecal material,² and are an important nutrient source for the gut microbiota. A wide range of carbohydrates are represented on intestinal epithelial cells, including polysaccharides, glycoproteins and glycolipids. *B. vulgatus* is a widespread member of the human microbiota, and is generally considered beneficial, although it is an occasional opportunistic pathogen. *B. vulgatus* is typically present at levels of around 4% of bacteria in the gut microbiota, but can rise to constitute >40% of the gut microflora in Crohn's disease patients.³ *B. vulgatus*, like other *Bacteroides* spp., possesses specialized polysaccharide utilization loci (PULs) encoding complex enzymatic machineries able to degrade and harness a wide variety of complex dietary polysaccharides along with SusC/SusD orthologues capable of importing oligosaccharide fragments into the periplasm.⁴ In addition, *B. vulgatus* and other members

of the Bacteroidetes have specialised PULs for the degradation of intestinal mucosal glycoproteins and the glycocalyx.⁵ However, it appears that the ability of *Bacteroides* spp. to degrade host glycoconjugates is also enabled by enzymes encoded outside of the PULs. *B. vulgatus* encodes a single copy of an enzyme from glycoside hydrolase family GH123,⁹ a poorly characterized family with an emerging ability to degrade host-derived glycoconjugates. In this work we demonstrate that previously uncharacterized protein BvGH123 is a *N*-acetyl- β -galactosaminidase. We experimentally demonstrate for the first time that a member of this family hydrolyses glycosides with retention of anomeric stereochemistry, and provide evidence for a neighbouring group participation mechanism through an X-ray crystal structure in complex with an inhibitor that mimics the proposed intermediate of the reaction mechanism.

Previous studies of GH123 members, initially NagP from *Paenibacillus* sp.,⁶ and CpNga123 from *C. perfringens* (whose structure was recently solved)⁷ have led to the proposal of a two-step neighbouring group participation mechanism for catalysis (Fig. 1). According to such a mechanism, the enzyme possesses two key active site residues acting in the role of acid/base and transition state stabilization.⁸ In the first step, nucleophilic attack by the 2-acetamido group oxygen on the anomeric centre, assisted by charge stabilization and orientation by the transition state stabilizing residue, occurs simultaneously with protonation of the glycosidic oxygen by the acid/base residue to assist leaving group departure, resulting in the formation of an oxazolinium ion. In the second step, the acid/base residue acts as a base to assist in deprotonation of a nucleophilic water molecule, while the stabilizing residue facilitates ring-opening of the oxazolinium ion intermediate.⁹ Evidence in support of this mechanism was initially based on the nanomolar inhibition of NagP by Gal-thiazoline;⁶ an inhibitor that mimics the proposed oxazolinium ion intermediate (more formally a closely-related transition-state),¹⁰ along with the proposal of a catalytic diad of adjacent carboxyl residues reminiscent of those seen in β -hexosaminidases of GH20 and GH84, which are known to act through a neighbouring group participation mechanism.^{11,12} Recently, the first X-ray structure of a

^a Department of Chemistry, University of York, Heslington, York, UK.
E-mail: gideon.davies@york.ac.uk

^b School of Chemistry and Bio21 Molecular Science and Biotechnology Institute, University of Melbourne, Parkville, Victoria, Australia.
E-mail: sjwill@unimelb.edu.au

^c ACRF Chemical Biology Division, The Walter and Eliza Hall Institute of Medical Research, Parkville, Victoria, Australia. E-mail: goddard-borger.e@wehi.edu.au

^d Department of Medical Biology, University of Melbourne, Parkville, Victoria, Australia

† Electronic supplementary information (ESI) available: SI figures, cloning, expression, biochemistry, and crystallography methods. See DOI: 10.1039/c6cc04649e



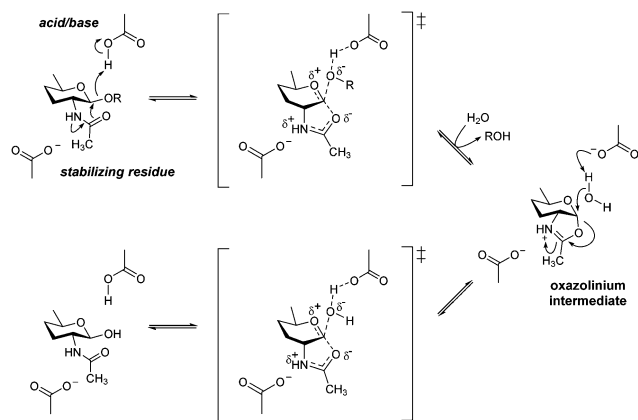


Fig. 1 Neighbouring group participation mechanism by a retaining N-acetyl-β-hexosaminidase. Hydroxyl groups have been omitted for clarity.

GH123 enzyme, *CpNga123*, in a product complex and a pseudo-Michaelis complex of an inactive mutant with substrate confirmed the identity of the catalytic diad, and revealed binding orientations of the 2-acetamido group that while not oriented directly below C1, was positioned in a manner consistent with that needed for neighbouring group participation.⁷

To further investigate the mechanism of the GH123 galactosaminidases, residues 20–582 of ABR39589.1, encoding BVU_2198, without its signal peptide (hereafter *BvGH123*) was expressed in *E. coli* (Fig. S1, ESI†). Size exclusion chromatography-multi-angle laser light scattering revealed *BvGH123* to be a dimer in solution. The enzyme displays a pH optimum of 5 using 4-nitrophenyl N-acetyl-β-D-galactosaminide (PNPGalNAc, 1) as a substrate (Fig. S2a, ESI†). The kinetic preference for β-galactosaminides versus β-glucosaminides was determined using PNPGalNAc and 4-nitrophenyl N-acetyl-β-D-glucosaminide (PNPGlcNAc). For PNPGalNAc, $k_{\text{cat}}/K_M = 8.0 \pm 0.4 \times 10^3 \text{ M}^{-1} \text{ s}^{-1}$ and for PNPGlcNAc, $k_{\text{cat}}/K_M = 3.8 \pm 0.6 \times 10^2 \text{ M}^{-1} \text{ s}^{-1}$; saturation could not be achieved, preventing the accurate determination of k_{cat} and K_M values. These data indicate a 21-fold preference for β-galactosaminides, consistent with previous reports on NagP⁶ and *CpNga123*,⁷ providing further evidence that the enzymes of this family are dedicated N-acetyl-β-galactosaminidases.

Previous studies have only speculated on the stereochemical outcome of substrate hydrolysis, which is of obvious importance for proposal of a feasible enzymatic mechanism.¹³ We used ¹H NMR spectroscopy to monitor the stereochemical outcome of the enzyme-catalyzed hydrolysis of PNPGalNAc (1) (Fig. 2). Upon addition of enzyme, rapid consumption of substrate led to the production of a new product, with an anomeric signal at δ 4.63 ppm that displayed a large ($J = 8 \text{ Hz}$) coupling constant. Over time, mutarotation led to the formation of a mixture of the first compound, and a new compound with an anomeric signal at δ 5.22 ppm characterized by a small ($J = 4 \text{ Hz}$) coupling constant. These experimental data are consistent with the initial formation of β-GalNAc (2β), revealing that *BvGH123*, and by inference all GH123 members, act with a net retention of anomeric configuration. Using isothermal titration calorimetry, Gal-thiazoline¹⁴ was shown to bind *BvGH123* with $K_D = 9.6 \text{ nM}$ (Fig. S2b, ESI†).

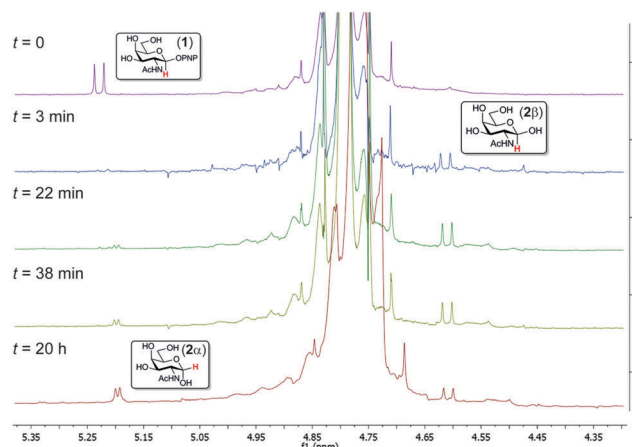


Fig. 2 Stacked ¹H NMR spectra showing time course of *BvGH123* hydrolysis of PNPGalNAc. Substrate hydrolysis results in initial release of β-GalNAc with retention of anomeric configuration, which then undergoes mutarotation.

Collectively, these results support previous suggestions that enzymes of family GH123 use a neighbouring group participation mechanism involving the 2-acetamido group.

At the time of our structure solution, no GH123 structure had been reported and thus the three-dimensional structure of *BvGH123* was solved by experimental phasing using single anomalous diffraction from a selenomethionine-substituted derivative and subsequently refined against a native dataset to a resolution of 1.85 Å (Table 1 and Table S1, ESI†). The overall structure reveals a two domain structure with an N-terminal β-sheet domain (residues 1–195) followed by a catalytic (β/α)₈-barrel domain (residues 196–563) (Fig. 3a). The latter has three insertions forming a 4-stranded β-wing domain and a C-terminal α-helical cap, as observed recently in the *CpGH123* structure.⁷ Structures of *BvGH123* and *CpNga123* overlap with an r.m.s.d. of approximately 1.7 Å over 500 residues. Differences include a longer N-terminus for *BvGH123*, and a C-terminal β-strand insertion followed by a longer C-terminal helix for *CpNga123*. Additionally a disulfide bond joining Cys117 and Cys430 is observed only in *BvGH123*, connecting the loop comprising residues 110–120 with the 430-loop which is part of the active site. Sequence conservation within the GH123 family is relatively low and is mainly confined to the catalytic residues and sections of the (β/α)₈-barrel. The N-terminal β-sheet domain, found in both structures, shows weak structural similarity to the IgG-fold found in several antigens and adhesion modules,

Table 1 3-D structure data for *BvGH123*

	Native (apo)	<i>BvGH123</i> –GalNAc	<i>BvGH123</i> –Gal-thiazoline
Space group	$P2_12_12_1$	$P2_12_12_1$	$P2_12_12_1$
Resolution limit	1.85 Å	2.1 Å	2.3 Å
R_{merge}	0.141(1.930)	0.104(1.530)	0.063(1.552)
$I/\sigma I$	9.9(1.2)	12.0(1.2)	15.6(1.1)
Completeness (%)	99.9(100)	100(100)	93.4(63.6)
R.m.s.d bond lengths (Å)	0.016	0.014	0.013
R.m.s.d bond angles (°)	1.70	1.59	1.63



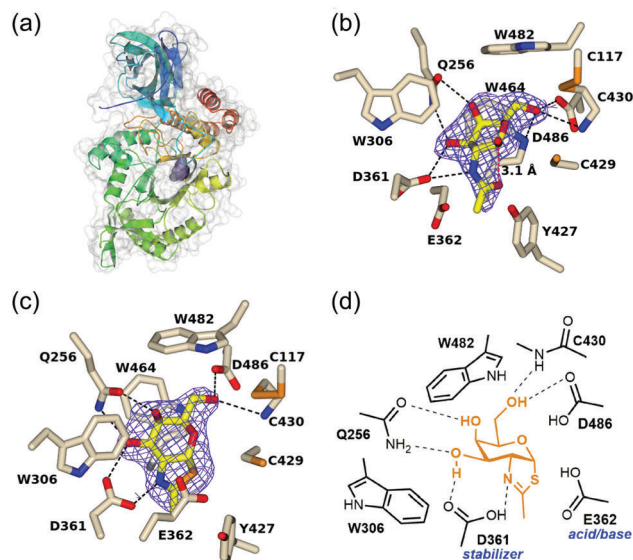


Fig. 3 Structures of *Bacteroides vulgatus* GH123 and complexes with Gal-thiazoline and GalNAc. (a) Overview of the *BvGH123* structure in complex with Gal-thiazoline, rainbow-coloured from the N- to C-terminus; Gal-thiazoline is shown as space filled van der Waals surface. Views of the active site of *BvGH123* in complex with (b) GalNAc and (c) Gal-thiazoline, highlighting the active site residues. The $2mF_o - DF_c$ map for GalNAc in blue is contoured at $0.22 \text{ e } \text{\AA}^{-3}$ (1σ r.m.s.d.) and $0.25 \text{ e } \text{\AA}^{-3}$ (1.5σ r.m.s.d.) for Gal-thiazoline. The C1–O interaction of the *N*-acetyl group in the GalNAc complex is highlighted with a red dotted line. (d) Interaction plot of Gal-thiazoline within the active site.

as well as within Titin, and might facilitate adhesion to the cell surface of the host, helping to degrade cell surface glycans.^{15a} Remote structural similarity is also observed for the BACON-domain found, for example, in GH5 enzymes.⁵ A stable assembly in the crystal lattice identified by PISA¹⁶ is formed by interaction of the 4-stranded β -wing domain formed by insertions between the second and third strands and the helix of the $(\beta/\alpha)_8$ -barrel (Fig. S3, ESI[†]), presumably representing the dimer observed in solution.

To gain insight into the structural basis of the retaining mechanism of *BvGH123*, we solved structures of complexes with the product GalNAc (Fig. 3b), as well as Gal-thiazoline at resolutions of 2.1 and 2.3 Å, respectively (Fig. 3c). Compared to the “apo” form, both complexes revealed a movement both of several of the loops lining the active site and of key residues, which is most pronounced for W306 and the adjacent pair of catalytic residues D361 and E362 (Fig. 4 and Fig. S4, ESI[†]). Similar movements were observed for *CpNGa123* upon engagement with carbohydrate.⁷ In the case of *BvGH123* upon binding to Gal-thiazoline the loop containing D361 and E362 moves to engage these acidic side chains into a closed conformation in which the catalytic residues engage in close contacts with the inhibitor. As the inhibitor is a mimic of the oxazolinium intermediate (or possibly the transition state),^{15b} these interactions appear to represent those of a catalytically competent form of the enzyme.

The X-ray structures of the inhibitor and product complexes of *BvGH123* provide an intimate view of the geometry of the

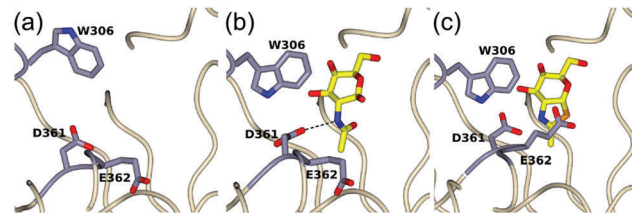


Fig. 4 *BvGH123* undergoes conformational changes upon ligand binding. Comparison of the conformations for the active site residues in: (a) fully open form of apo *BvGH123*; (b) partially closed form in complex with GalNAc; (c) fully closed form in complex with Gal-thiazoline.

active site. In the *BvGH123*–Gal-thiazoline complex, which is in a fully closed state, the adjacent carboxyl residues D361 and E362 adopt positions consistent with roles as transition state stabilizer and acid/base, respectively (Fig. 3c). The *BvGH123*–GalNAc product complex revealed only a partially closed conformation with W306 nestled above the pyranose and D361 engaging with the acetamido group of GalNAc (Fig. 3b). This complex contrasts with that reported for GalNAc bound to *CpNGa123*, which is in an open conformation (Fig. S4, ESI[†]).⁷ The pyranose ring of Gal-thiazoline adopts a 4C_1 conformation consistent with an expected ${}^1S_3 \rightarrow {}^4H_3 \rightarrow {}^4C_1$ conformational itinerary for the glycosylation half-reaction.¹⁷ Complexes of *CpNGa123*–D344N/E345Q with substrate (ganglioside glycans GA2 or Gb4) were observed in a 4C_1 conformation, which is inconsistent with the substrate distortion expected with a pseudo-axial orientation of the anomeric group, as anticipated for stereo-electronic reasons.⁷ Combined with the location of the 2-acetamido group away from C1, the Michaelis complexes obtained with *CpNGa123* have been suggested to represent non-catalytically-competent complexes in which the open conformation prevents the active centre residues from fully engaging with the substrate.

A comparison of the active sites of GH families that are known to utilise a substrate-assisted retaining mechanism, which includes families 18, 20, 25, 84 and 85, reveal a remarkable spatial conservation of the catalytic residues located on the fourth β -strand of the respective $(\beta/\alpha)_8$ -barrel (Fig. 5). Families GH20 and 84, like GH123, have the catalytic acid/base and stabilizer adjacent in their protein chains, and have essentially identical arrangements of these groups and the linking peptide backbone. Families GH18, 25 and 85 have a one residue insertion between the catalytic residues, yet still adopt a remarkably similar spatial arrangement. Likewise the active site closure motion now observed for two GH123 enzymes is also seen for a GH20 hexosaminidase and a GH84 O-GlcNAcase.^{7,12,22} These hexosaminidase families have little or no sequence conservation yet display similar folds and arrangement of catalytic residues and use a neighbouring group participation mechanism, suggesting a common solution to the chemical problem of hydrolysis of *N*-acetyl- β -hexosaminides.²³

This work was supported by the Australian Research Council (FT130100103), and the BBSRC (BB/K003836/1), and the Ramaciotti Foundation and VESKI with additional support from the Australian Cancer Research Foundation and Victorian State Government Operational Infrastructure Support, NHMRC IRISS



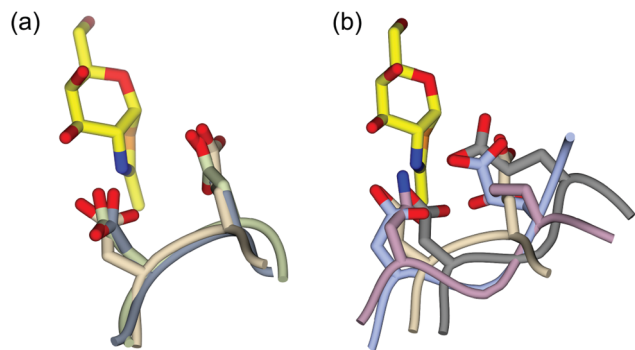


Fig. 5 Overlay of BvGH123–Gal-thiazoline active site residues (wheat) with members of other neighbouring group participation enzyme families (GH18, 20, 25, 84, 85). (a) Overlay of family representatives with adjacent catalytic residues: GH20 *Paenibacillus* sp. β -HexNAcase (purple, PDB: 3SUR),¹⁸ and GH84 *Bacteroides thetaiotaomicron* O-GlcNAcase (light green, PDB: 2CHN).¹¹ (b) Overlay of family representatives with non-adjacent catalytic residues: GH18 *Serratia marcescens* chitinase A (grey, PDB: 2WK2),¹⁹ GH25 *Aspergillus fumigatus* lysozyme (steel blue, PDB: 2X8R),²⁰ and GH85 *Streptococcus pneumoniae* endo-D (plum, PDB: 2W92).²¹

grant 9000220. We thank the Diamond Light Source for access to beamlines I02, I03 and I04 (proposal number mx-9948) that contributed to the results presented here. We also thank Dr Andrew Leech at the Bioscience Technology Facility in the Department of Biology in York for his help with the SEC-MALLS experiments. We are grateful to Dr Johan Turkenburg and Sam Hart for assistance during data collection and Wendy Offen for help with the crystallisation.

Notes and references

- P. G. Falk, L. V. Hooper, T. Midtvedt and J. I. Gordon, *Microbiol. Mol. Biol. Rev.*, 1998, **62**, 1157.
- D. P. Bojanova and S. R. Bordenstein, *PLoS Biol.*, 2016, **14**, e1002503.
- J. G. H. Ruseler-van Embden, R. van der Helm and L. M. C. van Lieshout, *FEMS Microbiol. Lett.*, 1989, **58**, 37.
- (a) B. A. White, R. Lamed, E. A. Bayer and H. J. Flint, *Annu. Rev. Microbiol.*, 2014, **68**, 279; (b) N. Terrapon, V. Lombard, H. J. Gilbert and B. Henrissat, *Bioinformatics*, 2015, **31**, 647; (c) J. Larsbrink, T. E. Rogers, G. R. Hemsworth, L. S. McKee, A. S. Tauzin, O. Spadiut, S. Kliner, N. A. Pudlo, K. Urs, N. M. Koropatkin, A. L. Creagh, C. A. Haynes, A. G. Kelly, S. N. Cederholm, G. J. Davies, E. C. Martens and H. Brumer, *Nature*, 2014, **506**, 498; (d) J. Larsbrink, A. J. Thompson, M. Lundqvist, J. G. Gardner, G. J. Davies and H. Brumer, *Mol. Microbiol.*, 2014, **94**, 418; (e) G. R. Hemsworth, G. Dejean, G. J. Davies and H. Brumer, *Biochem. Soc. Trans.*, 2016, **44**, 94.
- N. A. Pudlo, K. Urs, S. S. Kumar, J. B. German, D. A. Mills and E. C. Martens, *mBio*, 2015, **6**, e01282.
- T. Sumida, K. Fujimoto and M. Ito, *J. Biol. Chem.*, 2011, **286**, 14065.
- I. Noach, B. Pluinage, C. Laurie, K. T. Abe, M. G. Alteen, D. J. Vocadlo and A. B. Boraston, *J. Mol. Biol.*, 2016, **428**, 3253.
- D. J. Vocadlo and G. J. Davies, *Curr. Opin. Chem. Biol.*, 2008, **12**, 539.
- S. J. Williams, B. Mark, D. J. Vocadlo, M. N. James and S. G. Withers, *J. Biol. Chem.*, 2002, **277**, 40055.
- (a) M. S. Macauley, G. E. Whitworth, A. W. Debowski, D. Chin and D. J. Vocadlo, *J. Biol. Chem.*, 2005, **280**, 25313; (b) G. E. Whitworth, M. S. Macauley, K. A. Stubbs, R. J. Dennis, E. J. Taylor, G. J. Davies, I. R. Greig and D. J. Vocadlo, *J. Am. Chem. Soc.*, 2007, **129**, 635.
- R. J. Dennis, E. J. Taylor, M. S. Macauley, K. A. Stubbs, J. P. Turkenburg, S. J. Hart, G. N. Black, D. J. Vocadlo and G. J. Davies, *Nat. Struct. Mol. Biol.*, 2006, **13**, 365.
- M. Robb, C. S. Robb, M. A. Higgins, J. K. Hobbs, J. C. Paton and A. B. Boraston, *J. Biol. Chem.*, 2015, **290**, 30888.
- (a) E. C. Lai and S. G. Withers, *Biochemistry*, 1994, **33**, 14743; (b) S. Drouillard, S. Armand, G. J. Davies, C. E. Vorgias and B. Henrissat, *Biochem. J.*, 1997, **328**, 945; (c) B. L. Mark, D. J. Vocadlo, S. Knapp, B. L. Triggs-Raine, S. G. Withers and M. N. G. James, *J. Biol. Chem.*, 2001, **276**, 10330.
- S. Knapp and D. S. Myers, *J. Org. Chem.*, 2002, **67**, 2995.
- (a) F. Bäckhed, R. E. Ley, J. L. Sonnenburg, D. A. Peterson and J. I. Gordon, *Science*, 2005, **307**, 1915; (b) N. Cekic, J. E. Heinonen, K. A. Stubbs, C. Roth, Y. He, A. J. Bennet, E. J. McEachern, G. J. Davies and D. J. Vocadlo, *Chem. Sci.*, 2016, **7**, 3742.
- E. Krissinel, *Nucleic Acids Res.*, 2015, **43**, W314.
- Y. He, M. S. Macauley, K. A. Stubbs, D. J. Vocadlo and G. J. Davies, *J. Am. Chem. Soc.*, 2010, **132**, 1807.
- T. Sumida, K. A. Stubbs, M. Ito and S. Yokoyama, *Org. Biomol. Chem.*, 2012, **10**, 2607.
- J. M. Macdonald, C. A. Tarling, E. J. Taylor, R. J. Dennis, D. S. Myers, S. Knapp, G. J. Davies and S. G. Withers, *Angew. Chem., Int. Ed.*, 2010, **49**, 2599.
- J. E. Korczynska, S. Danielsen, U. Schagerlof, J. P. Turkenburg, G. J. Davies, K. S. Wilson and E. J. Taylor, *Acta Crystallogr., Sect. F: Struct. Biol. Cryst. Commun.*, 2010, **66**, 973.
- D. W. Abbott, M. S. Macauley, D. J. Vocadlo and A. B. Boraston, *J. Biol. Chem.*, 2009, **284**, 11676.
- J. F. Darby, J. Landstrom, C. Roth, Y. He, G. J. Davies and R. E. Hubbard, *Angew. Chem., Int. Ed. Engl.*, 2014, **53**, 13419.
- R. R. Copley and P. Bork, *J. Mol. Biol.*, 2000, **303**, 627; A. D. Goldman, J. T. Beatty and L. F. Landweber, *J. Mol. Evol.*, 2016, **82**, 17.

